European Journal of Mechanics B/Fluids 39 (2013) 1–10

Contents lists available at SciVerse ScienceDirect

European Journal of Mechanics B/Fluids

journal homepage: www.elsevier.com/locate/ejmflu

Remarks on the stability of the Navier–Stokes equations supplemented with stress boundary conditions

J.-L. Guermond [a,b,c], J. Léorat [d], F. Luddens [a,b,c], C. Nore [a,b,e,*]

[a] Laboratoire d'Informatique pour la Mécanique et les Sciences de l'Ingénieur, CNRS UPR 3251, BP 133, 91403 Orsay cedex, France
[b] Université Paris-Sud 11, France
[c] Department of Mathematics, Texas A&M University 3368 TAMU, College Station, TX 77843-3368, USA
[d] LUTH, Observatoire de Paris-Meudon, place Janssen, 92195-Meudon, France
[e] Institut Universitaire de France, 103 Bd Saint-Michel, 75005 Paris, France

ARTICLE INFO

Article history:
Received 16 January 2012
Received in revised form
5 July 2012
Accepted 17 November 2012
Available online 5 December 2012

Keywords:
Navier–Stokes equations and axisymmetric domains
Stress boundary conditions
Precession and Coriolis force

ABSTRACT

The purpose of this note is to analyze the long term stability of the Navier–Stokes equations augmented with the Coriolis force and supplemented stress boundary conditions. It is shown that spurious stability behaviors can occur depending whether the Coriolis force is active or not when the flow domain is axisymmetric.

1. Introduction

The liquid core of the Earth is often modeled as a heated conducting fluid enclosed between the solid inner core and the mantle. Numerically simulating the dynamics of the liquid core is difficult in many respects; one of the difficulties comes from the presence of viscous layers that develop at the boundaries of the fluid domain, i.e., the so-called inner core boundary (ICB) and core–mantle boundary (CMB). It is a common practice in the geophysics literature to use stress-free boundary conditions in order to minimize the role played by the viscous layers. Although this choice of boundary condition is convenient, it is not clear that it is more physically justified than using the no-slip condition. Actually, enforcing either the no-slip or the stress-free boundary condition may lead to significantly different results when it comes to simulating the geodynamo. For example, Glatzmaier and Roberts [1] and Kuang and Bloxham [2,3] have used the above two different sets of boundary conditions and have reported numerical buoyancy-driven dynamos in rapidly rotating spherical shells that differ in some fundamental aspects, see e.g. [4]. The simulations reported in [2] use the stress-free condition whereas those reported in [1] use the no-slip condition. The dynamo simulated in [2] has a magnetic field outside the core–mantle boundary that is dominated by an axial dipole component, like that of the Earth, and its intensity is close to the present geomagnetic dipole moment. The internal magnetic field outside the core–mantle boundary is comparable to that obtained by Glatzmaier and Roberts [1], but important differences in the velocity and magnetic fields between these two dynamos can be observed within the outer core and the Taylor–Proudman tangent cylinder. (It is known that rotation of the Earth rigidifies the flow field in the direction parallel to the rotation axis through a mechanism known as the Taylor–Proudman effect. This effect makes the imaginary cylinder that is tangent to the equator of the solid inner core and whose axis is parallel to the rotation axis of the Earth act like a solid boundary.) In the dynamo reported in [2] the fluid flow is almost stagnant inside the tangent cylinder and has a strong azimuthal component outside; the magnetic field is active throughout the outer core and is composed of two opposite toroidal cells and a simple dipolar poloidal structure. In the dynamo reported in [1] the fluid flow is composed of an intense polar vortex that is located inside the tangent cylinder and extends in the two hemispheres; the toroidal component of the magnetic field is active only inside the tangent cylinder and is concentrated near the ICB; the poloidal component has a complicated dipolar structure with extra closed loops near the ICB. It is suggested in [4] that the significantly

* Corresponding author at: Laboratoire d'Informatique pour la Mécanique et les Sciences de l'Ingénieur, CNRS UPR 3251, BP 133, 91403 Orsay cedex, France. Tel.: +33 1 69 85 80 90; fax: +33 1 69 85 80 88.
E-mail address: nore@limsi.fr (C. Nore).

0997-7546/$ – see front matter © 2012 Elsevier Masson SAS. All rights reserved.
doi:10.1016/j.euromechflu.2012.11.003

different structures of the above two dynamos should be attributed to the nature of the boundary conditions that are imposed at the ICB and CMB interfaces. Note finally that different thermal boundary conditions (i.e., fixed temperature or fixed heat-flux boundary conditions) lead also to different magnetic and fluid solutions [5].

In addition to thermal or compositional convection due to buoyancy, precession is also believed to be a possible source of energy for the geodynamo. The precession hypothesis has been formulated for the first time in [6] and experimentally investigated using a water model in [7]. It has since then been actively studied from the theoretical, experimental and numerical perspectives. However, it seems that it is only recently that numerical examples of precession dynamos have been reported in spheres [8,9], in spheroidal cavities [10] and in cylinders [11]. Recently, Wu and Roberts [10] have numerically studied the dynamo effect in a precessing oblate spheroid. To facilitate their analysis the authors have split the total velocity field into a basic stationary analytic (polynomial) solution (the so-called Poincaré flow) and a fluctuating part. Following ideas of Kerswell and Mason [12], they have implemented the stress-free boundary condition on the fluctuating component of the velocity in order to reduce the impact of the viscous layers at the rigid boundaries.

The purpose of the present paper is to show that the use of stress boundary conditions poses mathematical difficulties. We prove for instance that, if the fluid domain is not axisymmetric, the flow always returns to rest for large times when the stress-free boundary condition is enforced (see Proposition 2.1), but this may not be the case when the flow domain is axisymmetric (see Proposition 2.3). Various scenarios can occur depending whether the domain undergoes precession or not.

The note is organized as follows. We analyze the stress-free boundary condition in general fluid domains in Section 2. We show that this boundary condition is admissible if and only if the domain is not axisymmetric (see Proposition 2.2). We revisit the same question in axisymmetric domains that undergo precession in Sections 3 and 4. We show in Section 3 that the problem exhibits a spurious stability behavior if the stress-free condition is enforced on the velocity field minus the Poincaré flow (i.e., on the perturbation to the Poincaré flow; see Proposition 3.1). We show in Section 4 that the problem always returns to rest for large times if the homogeneous stress-free boundary condition is enforced. The theoretical argumentation developed in Sections 3 and 4 is numerically illustrated in Section 5. Concluding remarks are reported in Section 6.

2. Stress-free boundary condition without precession

The objective of this section is to investigate the long term stability of the Navier–Stokes equations equipped with the stress-free boundary condition. The fluid domain is denoted Ω and is assumed to be open, bounded and Lipschitz.

2.1. Position of the problem

We are interested in the motion of an incompressible fluid in a container Ω with boundary Γ. The container is assumed to be at rest in an inertial reference frame. Denoting $\mathbf{u}$ the velocity of the fluid and p the pressure, the fluid motion is modeled by means of the incompressible Navier–Stokes equations:

$$\partial_t \mathbf{u} + \mathbf{u}\cdot\nabla\mathbf{u} - 2\nu\nabla\cdot\boldsymbol{\epsilon}(\mathbf{u}) + \nabla p = 0, \tag{2.1}$$

$$\nabla\cdot\mathbf{u} = 0, \tag{2.2}$$

$$\mathbf{u}_{|t=0} = \mathbf{u}_0, \tag{2.3}$$

where ν is the kinematic viscosity, $\boldsymbol{\epsilon}(\mathbf{u}) := \frac{1}{2}\left(\nabla\mathbf{u} + \nabla\mathbf{u}^T\right)$ is the strain rate tensor, and $\mathbf{u}_0$ is an initial data in $\mathbf{H} := \{\mathbf{v}\in\mathbf{L}^2(\Omega) : \nabla\cdot\mathbf{v} = 0,\ \mathbf{v}\cdot\mathbf{n}_{\Gamma} = 0\}$. It is a common practice to replace the term $\nabla\cdot\left(\nabla\mathbf{u}+\nabla\mathbf{u}^T\right)$ in the momentum equation by $\Delta\mathbf{u}$ since $\nabla\cdot\nabla\mathbf{u}^T = 0$ for incompressible flows. We nevertheless keep the original form of the viscous stress since we want to enforce the so-called stress-free boundary condition:

$$(\mathbf{n}\cdot\boldsymbol{\epsilon}(\mathbf{u}))\times\mathbf{n}_{|\Gamma} = 0, \tag{2.4}$$

together with the impenetrable boundary condition:

$$\mathbf{n}\cdot\mathbf{u}_{|\Gamma} = 0, \tag{2.5}$$

where $\mathbf{n}$ is the unit outward normal on Γ. The stress-free condition means that the tangent component of the stress at the boundary is zero. We shall see that this boundary condition is admissible in general for non-axisymmetric domains, but it yields pathological stability behaviors if the fluid domain is a solid of revolution.

We are not going to discuss the well-posedness of the above problem in its full generality since it is still unknown whether the three-dimensional Navier–Stokes equations are well-posed under the much simpler no-slip boundary condition. We nevertheless recognize as a symptom of pathological stability behavior the fact that there are solutions to (2.1)–(2.2)–(2.3)–(2.4)–(2.5) that do not return to rest as $t\to+\infty$ if Ω is axisymmetric.

Definition 2.1. We say that Ω is stress-free admissible if there is a constant $K>0$, possibly depending on Ω, so that the following holds

$$K\int_\Omega \mathbf{v}^2 \leqslant \int_\Omega \boldsymbol{\epsilon}(\mathbf{v}) : \boldsymbol{\epsilon}(\mathbf{v}),\quad \forall\mathbf{v}\in\mathbf{H}^1(\Omega),\ \mathbf{v}\cdot\mathbf{n}_{|\Gamma} = 0 \tag{2.6}$$

where ":" denotes the tensor double product.

Proposition 2.1. *Assume that Ω is stress-free admissible, then $\{0\}$ is the global attractor of (2.1)–(2.2)–(2.3)–(2.4)–(2.5).*

Proof. We omit the details concerning the existence of Leray–Hopf solutions, which can be constructed using standard Galerkin techniques [13–15], and we focus only on the aspects of the question which are relevant to our discussion. It is clear that $\{0\}$ is an invariant set of (2.1)–(2.2)–(2.3)–(2.4)–(2.5). Let $\mathbf{B}$ be a bounded set in $\mathbf{H}$ and let $\mathbf{u}_0\in\mathbf{B}$. Let $\mathbf{u}$ be a Leray–Hopf solution corresponding to the initial data $\mathbf{u}_0$ and let $\mathbf{v}$ be a smooth solenoidal vector field satisfying the impenetrable boundary condition. Upon multiplying the momentum equation by $\mathbf{v}$ and integrating over the domain we obtain

$$\int_\Omega \partial_t\mathbf{u}\cdot\mathbf{v} + \int_\Omega \mathbf{u}\cdot\nabla\mathbf{u}\cdot\mathbf{v} - 2\nu\int_\Omega \nabla\cdot\boldsymbol{\epsilon}(\mathbf{u})\cdot\mathbf{v} + \int_\Omega \nabla p\cdot\mathbf{v} = 0.$$

Solenoidality and the impenetrable boundary condition imply that $\int_\Omega \nabla p\cdot\mathbf{v} = -\int_\Omega p\nabla\cdot\mathbf{v} + \int_\Gamma p\mathbf{v}\cdot\mathbf{n} = 0$. Now, using the decomposition

$$\mathbf{v} = (\mathbf{n}\cdot\mathbf{v})\mathbf{n} - \mathbf{n}\times(\mathbf{n}\times\mathbf{v}),$$

and integrating by parts the viscous term we obtain:

$$\begin{aligned}
-\int_\Omega \nabla\cdot\boldsymbol{\epsilon}(\mathbf{u})\cdot\mathbf{v} &= \int_\Omega \boldsymbol{\epsilon}(\mathbf{u}) : \nabla\mathbf{v} - \int_\Gamma \mathbf{n}\cdot\boldsymbol{\epsilon}(\mathbf{u})\cdot\mathbf{v} \\
&= \int_\Omega \boldsymbol{\epsilon}(\mathbf{u}) : \boldsymbol{\epsilon}(\mathbf{v}) + \int_\Gamma (\mathbf{n}\cdot\boldsymbol{\epsilon}(\mathbf{u})\times\mathbf{n})\cdot(\mathbf{n}\times\mathbf{v}) \\
&= \int_\Omega \boldsymbol{\epsilon}(\mathbf{u}) : \boldsymbol{\epsilon}(\mathbf{v}).
\end{aligned}$$

The transport term is re-written in the following form

$$\int_\Omega \mathbf{u}\cdot\nabla\mathbf{u}\cdot\mathbf{v} = \int_\Omega \frac{1}{2}\nabla\cdot(\mathbf{u}(\mathbf{u}\cdot\mathbf{v})) + \frac{1}{2}\int_\Omega (\mathbf{u}\cdot\nabla\mathbf{u}\cdot\mathbf{v} - \mathbf{u}\cdot\nabla\mathbf{v}\cdot\mathbf{u}) = \frac{1}{2}\int_\Omega (\mathbf{u}\cdot\nabla\mathbf{u}\cdot\mathbf{v} - \mathbf{u}\cdot\nabla\mathbf{v}\cdot\mathbf{u}).$$

We now apply the above identities by replacing $\mathbf{v}$ by a sequence $\{\mathbf{v}_n\}_{n\in\mathbb{N}}$ that converges in the appropriate norm to $\mathbf{u}$. By integrating in time over an arbitrary interval (t_1, t_2) and by passing to the limit (we omit the details again, see Sell [15, Section 2.3]), we finally obtain

$$\frac{1}{2}\int_\Omega \mathbf{u}^2(t_2,\mathbf{x})\,\mathrm{d}\mathbf{x} + 2\nu\int_{t_1}^{t_2}\int_\Omega \boldsymbol{\epsilon}(\mathbf{u}):\boldsymbol{\epsilon}(\mathbf{u})\,\mathrm{d}\mathbf{x}\,\mathrm{d}\tau \le \frac{1}{2}\int_\Omega \mathbf{u}^2(t_1,\mathbf{x})\,\mathrm{d}\mathbf{x}. \tag{2.7}$$

Note that equality is lost in the passage to the limit. Then using (2.6), we infer the following inequality:

$$\frac{1}{2}\int_\Omega \mathbf{u}^2(t_2,\mathbf{x})\,\mathrm{d}\mathbf{x} + 2K\nu\int_{t_1}^{t_2}\int_\Omega \mathbf{u}^2\,\mathrm{d}\mathbf{x}\,\mathrm{d}\tau \leqslant \frac{1}{2}\int_\Omega \mathbf{u}^2(t_1,\mathbf{x})\,\mathrm{d}\mathbf{x},$$

which, owing to the Gronwall lemma (see Lemma 4.1), immediately leads to $\|\mathbf{u}\|_{\mathbf{L}^2(\Omega)} \leqslant \|\mathbf{u}_0\|_{\mathbf{L}^2(\Omega)}\mathrm{e}^{-2K\nu t}$, thereby proving that $\mathbf{u}\to 0$ as $t\to+\infty$. □

We shall see that the stress-free admissibility condition (2.6) does not hold for axisymmetric fluid domains, which are common in geoscience.

Remark 2.1. Note that whether equality holds in (2.7) in three space dimensions is an open question related to the Navier–Stokes Millennium Prize from the Clay institute. For this reason we refrain from invoking the time derivative of the kinetic energy in the proof of Proposition 2.1. The mapping $t \longmapsto \int_\Omega \mathbf{u}^2\,\mathrm{d}\mathbf{x}$ is a priori lower semi-continuous only, and, upon denoting $\mathbf{L}^2_w(\Omega)$ the space $\mathbf{L}^2(\Omega)$ equipped with the weak topology, the mapping $t \longmapsto \mathbf{u}\in\mathbf{L}^2_w(\Omega)$ is continuous.

2.2. The non-axisymmetric case

To better understand the stress-free admissibility condition (2.6), we first prove that it holds if and only if Ω is not axisymmetric.

Definition 2.2. We say that Ω is axisymmetric (or is a solid of revolution) if and only if there is a rotation $\mathbf{R}:\Omega\longrightarrow\Omega$ which is tangent on Γ.

Upon introducing the average operator over Ω, $\langle v\rangle := \frac{1}{|\Omega|}\int_\Omega v$, where $|\Omega|$ is the volume of Ω, the following lemma gives a characterization of non-axisymmetric domains:

Lemma 2.1 (*Desvillettes–Villani [16]*)**.** *Assume that the domain Ω is of class $\mathcal{C}^1$ but is not a solid of revolution, then there is $c>0$ so that*

$$c|\Omega|\langle\nabla\times\mathbf{v}\rangle^2 \le \|\boldsymbol{\epsilon}(\mathbf{v})\|_{\mathbf{L}^2(\Omega)}, \qquad \forall\mathbf{v}\in\mathbf{H}^1(\Omega),\ \mathbf{v}\cdot\mathbf{n}_{|\Gamma}=0.$$

We are now in measure to state the main result of this section:

Proposition 2.2. *Assume that the domain Ω is of class $\mathcal{C}^1$, then Ω is stress-free admissible if and only if Ω is not a solid of revolution.*

Proof. Let us assume first that Ω is not a solid of revolution. Let us now assume that (2.6) does not hold. We start from the Korn inequality (cf. e.g. [17]): there exists a constant $c>0$ such that, for all $\mathbf{v}\in\mathbf{H}^1(\Omega)$,

$$\|\mathbf{v}\|_{\mathbf{L}^2(\Omega)} + \|\nabla\mathbf{v}\|_{\mathbf{L}^2(\Omega)} \le c\left(\|\mathbf{v}\|_{\mathbf{L}^2(\Omega)} + \|\nabla\mathbf{v}+\nabla\mathbf{v}^T\|_{\mathbf{L}^2(\Omega)}\right). \tag{2.8}$$

Since (2.6) does not hold, for any $n\in\mathbb{N}$, one can find $\mathbf{u}_n\in\mathbf{H}^1(\Omega)$ such that

$$\mathbf{u}_n\cdot\mathbf{n}_{|\Gamma}=0, \qquad \|\mathbf{u}_n\|_{\mathbf{L}^2(\Omega)}=1, \quad\text{and}\quad \|\nabla\mathbf{u}_n+\nabla\mathbf{u}_n^T\|_{\mathbf{L}^2(\Omega)} \leqslant \frac{1}{n}.$$

The Korn inequality implies that the sequence $\mathbf{u}_n$ is bounded in $\mathbf{H}^1(\Omega)$. Since the inclusion $\mathbf{H}^1(\Omega)\subset\mathbf{L}^2(\Omega)$ is compact, there exists $\mathbf{u}\in\mathbf{H}^1(\Omega)$ such that (we keep using $\mathbf{u}_n$ after extraction of the converging sub-sequence) $\|\mathbf{u}_n-\mathbf{u}\|_{\mathbf{L}^2(\Omega)}\to 0$ and $\mathbf{u}_n\rightharpoonup\mathbf{u}$ in $\mathbf{H}^1(\Omega)$. We also have

$$\nabla\mathbf{u}_n+\nabla\mathbf{u}_n^T\to 0 \text{ in } \mathbf{L}^2(\Omega) \quad\text{and}$$
$$\nabla\mathbf{u}_n+\nabla\mathbf{u}_n^T\to\nabla\mathbf{u}+\nabla\mathbf{u}^T \text{ in } \mathcal{D}'(\Omega),$$

which finally gives $\nabla\mathbf{u}+\nabla\mathbf{u}^T=0$ ($\mathcal{D}(\Omega)$ is the space of smooth vector-valued functions with compact support in Ω and $\mathcal{D}'(\Omega)$ is the space of vector-valued distributions over Ω, i.e., the linear forms acting on $\mathcal{D}(\Omega)$.) Applying the Korn inequality to $\mathbf{u}-\mathbf{u}_n$ and using the fact that

$$\|\mathbf{u}_n-\mathbf{u}\|_{\mathbf{L}^2(\Omega)} + \|\nabla\mathbf{u}_n+\nabla\mathbf{u}_n^T-\nabla\mathbf{u}-\nabla\mathbf{u}^T\|_{\mathbf{L}^2(\Omega)}\to 0,$$

we infer that $\|\mathbf{u}_n-\mathbf{u}\|_{\mathbf{H}^1(\Omega)}\to 0$. This allows us to pass to the limit on the boundary condition $\mathbf{u}\cdot\mathbf{n}_{|\Gamma}=0$. The condition $\boldsymbol{\epsilon}(\mathbf{u})=0$ implies that there are two vectors $\mathbf{t}\in\mathbb{R}^3$, $\boldsymbol{\omega}\in\mathbb{R}^3$ so that $\mathbf{u}=\mathbf{t}+\boldsymbol{\omega}\times\mathbf{x}$. This means that $\nabla\times\mathbf{u}=\langle\nabla\times\mathbf{u}\rangle=\boldsymbol{\omega}$. Using Lemma 2.1, we conclude that $\boldsymbol{\omega}=0$, which means that $\mathbf{u}=\mathbf{t}$. The boundary condition $\mathbf{u}\cdot\mathbf{n}_{|\Gamma}=0$ implies $\mathbf{t}=0$; this in turn means $\mathbf{u}=0$, which is impossible because $\|\mathbf{u}\|_{\mathbf{L}^2(\Omega)}=1$. In conclusion, (2.6) holds.

Let us assume now that Ω is axisymmetric. This means that there is a rotation $\mathbf{R}:\Omega\longrightarrow\Omega$ which is tangent on Γ. Without loss of generality we assume that the rotation axis is parallel to $\mathbf{e}_z$ and the coordinate origin is located on this axis. Then $\mathbf{R}(\mathbf{x})=\omega\mathbf{e}_z\times\mathbf{x}$ and clearly $\mathbf{R}\in\mathbf{H}^1(\Omega)$, $\mathbf{R}(\mathbf{x})\cdot\mathbf{n}(\mathbf{x})_{|\Gamma}=0$, $\|\mathbf{R}\|_{\mathbf{L}^2(\Omega)}\neq 0$ but (2.6) does not hold since $\boldsymbol{\epsilon}(\mathbf{R})=0$. □

2.3. The axisymmetry curse

Let us assume that Ω is axisymmetric. We are going to show the following statement in this section.

Claim 2.1. *The zero velocity field, 0, is in the global attractor of (2.1)–(2.2)–(2.3)–(2.4)–(2.5), but the rest state, {0}, is not an attractor. There are initial data that create flows that never return to rest. In particular, if the initial data is a rigid-body rotation, the flow will rotate for ever without losing energy.*

Recall that it can be shown that Ω is axisymmetric if and only if Ω is either a sphere (and all the directions are symmetry axes) or Ω has a unique symmetry axis. Without loss of generality, we assume that Oz is the only symmetry axis of Ω. Recall that all the rigid-body rotations about Oz can be written as follows $\mathbf{x}\longmapsto\omega\mathbf{e}_z\times\mathbf{x}$, $\omega\in\mathbb{R}$, where $\mathbf{x}$ is the position vector. We introduce the following space

$$\mathcal{R} := \operatorname{span}\{\mathbf{e}_z\times\mathbf{x}\}, \tag{2.9}$$

and its orthogonal complement in $\mathbf{L}^2(\Omega)$, say $\mathcal{R}^\perp$.

Lemma 2.2. *Let Ω be an open, bounded, connected, domain of class $\mathcal{C}^1$ with unique symmetry axis Oz. There exists $K>0$ such that the following holds for every $\mathbf{v}\in\mathcal{R}^\perp\cap\mathbf{H}^1(\Omega)$ with $\mathbf{v}\cdot\mathbf{n}=0$:*

$$K\|\mathbf{v}\|^2_{\mathbf{L}^2(\Omega)} \le \int_\Omega |\boldsymbol{\epsilon}(\mathbf{v})|^2\,d\mathbf{x},$$

where we denote $|\boldsymbol{\epsilon}(\mathbf{v})|^2 := \boldsymbol{\epsilon}(\mathbf{v}):\boldsymbol{\epsilon}(\mathbf{v})$.

Proof. The proof is similar to that of Proposition 2.2 and proceeds by contradiction. We consider a sequence $\mathbf{v}_n \in \mathcal{R}^\perp \cap \mathbf{H}^1(\Omega)$ with vanishing normal component such that

$$\|\mathbf{v}_n\|_{\mathbf{L}^2} = 1 \quad \text{and} \quad \|\boldsymbol{\epsilon}(\mathbf{v}_n)\|_{\mathbf{L}^2} \leqslant \frac{1}{n}.$$

Using Korn's inequality, we can prove that (up to extraction) $\mathbf{v}_n$ converges in $\mathbf{H}^1(\Omega)$, and the limit $\mathbf{v}$ satisfies

$$\mathbf{v} \in \mathcal{R}^\perp, \qquad \mathbf{v}\cdot\mathbf{n} = 0 \quad \text{and} \quad \boldsymbol{\epsilon}(\mathbf{v}) = 0.$$

This implies that $\mathbf{v}$ is the sum of a translation plus a rigid-body rotation. But Ω being bounded the translation is zero. The unique symmetry axis of Ω being Oz, the condition $\mathbf{v}\cdot\mathbf{n} = 0$ implies that $\mathbf{v}$ is a rigid-body rotation about the Oz-axis, i.e., $\mathbf{v} \in \mathcal{R} \cap \mathcal{R}^\perp = \{0\}$, which contradicts $\|\mathbf{v}\|_{\mathbf{L}^2(\Omega)} = 1$. □

We claim that the Navier–Stokes problem (2.1)–(2.2) equipped with boundary conditions (2.4)–(2.5) has spurious stability properties due to the following proposition.

Proposition 2.3. (i) *$\mathcal{R}$ is the global attractor of* (2.1)–(2.2)–(2.3) – (2.4)–(2.5). (ii) *No element in $\mathcal{R}$ is an attractor.*

Proof. (i) Let $\mathbf{u} \in L^2((0,+\infty);\mathbf{L}^2(\Omega)) \cap L^\infty((0,+\infty);\mathbf{H}^1(\Omega))$ be a Leray–Hopf solution of (2.1)–(2.5) and consider the following decomposition:

$$\mathbf{u}(t) = \mathbf{u}^\perp(t) + \lambda(t)\mathbf{e}_z \times \mathbf{x}, \quad \text{where}$$
$$\mathbf{u}^\perp(t) \in \mathcal{R}^\perp,\ \lambda(t) \in \mathbb{R},\ \forall t \in [0,+\infty).$$

Invoking Lemma 3.1 we infer that $\frac{\mathrm{d}\lambda(t)}{\mathrm{d}t} = 0$, implying that $\lambda(t) = \lambda(0) := \lambda_0$. Let $t_2 > t_1 > 0$ be two positive times, then $\mathbf{u}$ being a Leray–Hopf solution implies that

$$\|\mathbf{u}^\perp(t_2)\|^2_{\mathbf{L}^2(\Omega)} + c_z\lambda(t_2)^2 + 4\nu\int_{t_1}^{t_2}\int_\Omega |\boldsymbol{\epsilon}(\mathbf{u})|^2\,\mathrm{d}\mathbf{x}\,\mathrm{d}\tau \le \|\mathbf{u}^\perp(t_1)\|^2_{\mathbf{L}^2(\Omega)} + c_z\lambda(t_1)^2,$$

where $c_z := \|\mathbf{e}_z \times \mathbf{x}\|^2_{\mathbf{L}^2(\Omega)}$. Since $\lambda(t_2) = \lambda(t_1)$, Lemma 2.2 implies

$$\|\mathbf{u}^\perp(t_2)\|^2_{\mathbf{L}^2(\Omega)} + 4\nu K\int_{t_1}^{t_2} \|\mathbf{u}^\perp\|^2_{\mathbf{L}^2(\Omega)}\,\mathrm{d}\tau \le \|\mathbf{u}^\perp(t_1)\|^2_{\mathbf{L}^2(\Omega)}.$$

Using the Gronwall–Bellman inequality (see Lemma 4.1), we infer that $\|\mathbf{u}^\perp(t)\|_{\mathbf{L}^2(\Omega)} \le \|\mathbf{u}_0\|_{\mathbf{L}^2(\Omega)}\mathrm{e}^{-2\nu K t}$.

In conclusion

$$\|\mathbf{u}(t) - \lambda_0\mathbf{e}_z \times \mathbf{x}\|_{\mathbf{L}^2(\Omega)} = \|\mathbf{u}^\perp(t)\|_{\mathbf{L}^2(\Omega)} \le \|\mathbf{u}_0\|_{\mathbf{L}^2(\Omega)}\mathrm{e}^{-2\nu K t}.$$

This implies that the global attractor, say $\mathcal{A}$, is such that $\mathcal{A} \subset \mathcal{R}$, but since λ_0 spans $\mathbb{R}$, we conclude that $\mathcal{A} = \mathcal{R}$.

(ii) Let us consider the rigid-body rotation field $\mathbf{u} = \omega\mathbf{e}_z \times \mathbf{x} \in \mathcal{R}$. It is clear that $\{\mathbf{u}\}$ is an invariant set, i.e., $\mathbf{u}$ is a steady-state solution. Let $\mathbf{B}(\mathbf{u},\rho) \in \mathbf{H}$ be the ball centered at $\mathbf{u}$ of arbitrary radius $\rho > 0$. Let $\mathbf{v} = \mu\mathbf{e}_z \times \mathbf{x} \in \mathcal{R}$, $\mu \neq 0$, be another rigid-body rotation and assume that μ is small enough so that $\mathbf{u}+\mathbf{v} \in \mathbf{B}(\mathbf{u},\rho)$. Clearly $\mathbf{u}+\mathbf{v}$ satisfies (2.2), (2.4), (2.5) (recall that $\boldsymbol{\epsilon}(\mathbf{u}+\mathbf{v}) = 0$). Let us observe that $\partial_t(\mathbf{u}+\mathbf{v}) - 2\nu\nabla\cdot(\boldsymbol{\epsilon}(\mathbf{u}+\mathbf{v})) = 0$ and

$$\begin{aligned}(\mathbf{u}+\mathbf{v})\cdot\nabla(\mathbf{u}+\mathbf{v}) &= 2(\mathbf{u}+\mathbf{v})\cdot\boldsymbol{\epsilon}(\mathbf{u}+\mathbf{v}) \\ &\quad - (\mathbf{u}+\mathbf{v})\cdot(\nabla(\mathbf{u}+\mathbf{v}))^T \\ &= -\frac{1}{2}\nabla|\mathbf{u}+\mathbf{v}|^2,\end{aligned}$$

since $\mathbf{u}+\mathbf{v}$ is a rigid-body rotation. Upon setting $p = \frac{1}{2}|\mathbf{u}+\mathbf{v}|^2$ we conclude that $\mathbf{u}+\mathbf{v}$ solves (2.1). This proves that $\mathbf{u}+\mathbf{v}$ is invariant (i.e., a steady-state solution). In other words $\mathbf{u}+\mathbf{v}$ does not converge to $\mathbf{u}$, no matter how small ρ is, thereby proving that the set $\{\mathbf{u}\}$ is not an attractor, no matter how large ν is. □

2.4. An admissible stress-free-like boundary condition

The principal motivation to consider the so-called stress-free boundary condition is that it minimizes viscous layers and is thus less computationally demanding than the no-slip boundary condition. We have seen above that it unfortunately leads to pathological stability properties when the computational domain is axisymmetric. One possible remedy to this problem is to consider the following non-symmetric boundary condition:

$$(\mathbf{n}\cdot\nabla\mathbf{u}) \times \mathbf{n}_{|\Gamma} = 0. \tag{2.10}$$

This condition expresses that the tangent components of the normal derivative of the velocity field are zero. The physical interpretation of this condition is definitely less appealing than that of the stress-free boundary condition. However (2.10) and the stress-free condition are equally numerically convenient. The main advantage we see in (2.10) over the stress-free condition is that it yields standard stability properties, i.e., $\{0\}$ is the global attractor.

Lemma 2.3. *The following holds for all smooth solenoidal vector field $\mathbf{u}$ that satisfies $(\mathbf{n}\cdot\nabla\mathbf{u}) \times \mathbf{n}_{|\Gamma} = 0$:*

$$\int_\Omega -\nabla\cdot(\boldsymbol{\epsilon}(\mathbf{u}))\cdot\mathbf{v} = \frac{1}{2}\int_\Omega \nabla\mathbf{u} : \nabla\mathbf{v}, \qquad \forall\mathbf{v} \in \mathbf{H}^1(\Omega),\ \mathbf{v}\cdot\mathbf{n}_{|\Gamma} = 0. \tag{2.11}$$

Proof. Upon observing that $\nabla\cdot(\boldsymbol{\epsilon}(\mathbf{u})) = \frac{1}{2}\nabla\cdot(\nabla\mathbf{u})$ since $\mathbf{u}$ is solenoidal, we infer that

$$\begin{aligned}\int_\Omega -\nabla\cdot(\boldsymbol{\epsilon}(\mathbf{u}))\cdot\mathbf{v} &= \int_\Omega -\frac{1}{2}\nabla\cdot(\nabla\mathbf{u})\cdot\mathbf{v} \\ &= \frac{1}{2}\int_\Omega \nabla\mathbf{u} : \nabla\mathbf{v} - \frac{1}{2}\int_\Gamma (\mathbf{n}\cdot\nabla\mathbf{u})\cdot\mathbf{v} \\ &= \frac{1}{2}\int_\Omega \nabla\mathbf{u} : \nabla\mathbf{v} - \frac{1}{2}\int_\Gamma (\mathbf{n}\cdot\nabla\mathbf{u})\cdot((\mathbf{n}\cdot\mathbf{v})\mathbf{n}) \\ &\quad + \frac{1}{2}\int_\Gamma ((\mathbf{n}\cdot\nabla\mathbf{u})\times\mathbf{n})\cdot(\mathbf{n}\times\mathbf{v}) \\ &= \frac{1}{2}\int_\Omega \nabla\mathbf{u} : \nabla\mathbf{v},\end{aligned}$$

where we used again the decomposition $\mathbf{v}_{|\Gamma} = (\mathbf{n}\cdot\mathbf{v})\mathbf{n} - \mathbf{n}\times(\mathbf{n}\times\mathbf{v})$. □

Proposition 2.4. *Assume that Ω is an open, connected, bounded Lipschitz domain, then $\{0\}$ is the global attractor of* (2.1)–(2.2)–(2.3) – (2.10)–(2.5).

Proof. Repeat the argument in the proof of Proposition 2.1 using Lemma 2.3 together with the following Poincaré-like inequality

$$K\int_\Omega \mathbf{v}^2 \le \int_\Omega |\nabla\mathbf{v}|^2, \qquad \forall\mathbf{v} \in \mathbf{H}^1(\Omega),\ \mathbf{v}\cdot\mathbf{n}_{|\Gamma} = 0,$$

which can be shown to hold by proceeding as in the proof of Proposition 2.2. □

3. Precession driven flow with Poincaré stress

If the fluid domain is a spheroid that undergoes precession, the time-independent Navier–Stokes equations supplemented with the impenetrable condition admit a so-called Poincaré solution. We show in this section that, independently of the value of the viscosity, the Poincaré solution is not an attractor of the problem if the tangential stress at the boundary is enforced to be equal to that of the steady-state Poincaré solution.

3.1. Geometry and equations

The container is an ellipsoid of revolution of center O and symmetry axis Oz. The unit vector along the Oz-axis is $\mathbf{e}_z$. The unit vectors along the other two orthogonal axes Ox and Oy are $\mathbf{e}_x$ and $\mathbf{e}_y$, respectively. The surface of the spheroid is defined by the equation

$$x^2 + y^2 + (1+\beta)z^2 = 1, \tag{3.1}$$

where $\beta > -1$ and $\beta \neq 0$. We assume that the Ox-axis is fixed in an inertial reference frame and the container rotates about the Ox-axis with angular velocity $\varepsilon\mathbf{e}_x$. The reference frame $(O, \mathbf{e}_x, \mathbf{e}_y, \mathbf{e}_z)$ is non-inertial, and the non-dimensional Navier–Stokes equations describing the motion of the fluid in this reference frame are written as follows:

$$\partial_t \mathbf{u} + \mathbf{u}\cdot\nabla\mathbf{u} - 2\nu\nabla\cdot\boldsymbol{\epsilon}(\mathbf{u}) + 2\varepsilon\mathbf{e}_x \times \mathbf{u} + \nabla p = 0, \tag{3.2}$$

$$\nabla\cdot\mathbf{u} = 0, \tag{3.3}$$

$$\mathbf{u}_{|t=0} = \mathbf{u}_0. \tag{3.4}$$

The only inertial effect to be considered in this frame is the Coriolis force induced by the rotation about the Ox-axis. Note that the definition of the pressure has been changed to account for the centripetal acceleration, $\varepsilon\mathbf{e}_x \times (\varepsilon\mathbf{e}_x \times \mathbf{x})$. We additionally enforce the impenetrable boundary condition,

$$\mathbf{u}\cdot\mathbf{n}_{|\Gamma} = 0. \tag{3.5}$$

The system (3.2)–(3.3)–(3.5) is known to admit a steady-state solution called the Poincaré flow (see e.g. [10]) whose expression is as follows:

$$\mathbf{u}_P = -y\mathbf{e}_x + \left(x - \frac{2\varepsilon}{\beta}(1+\beta)z\right)\mathbf{e}_y + \frac{2\varepsilon}{\beta}y\mathbf{e}_z. \tag{3.6}$$

Of course, $\mathbf{u}_P$ does not solve the Navier–Stokes system (3.2)–(3.3) equipped with the no-slip boundary condition. However, it has been shown formally in Stewartson and Roberts [18] that if the ellipsoid additionally rotates about the Oz-axis with angular velocity $\mathbf{e}_z$ and if $\nu \to 0$ and $\varepsilon \to 0$, the no-slip Navier–Stokes solution converges to $\mathbf{u}_P$ when $t \to +\infty$, except in thin Ekman layers on Γ. This result is the main reason why we are interested in the Poincaré solution.

One way to force $\mathbf{u}_P$ to be a Navier–Stokes solution consists of proceeding as in [10] and to consider the problem (3.2)–(3.3)–(3.5) equipped with the additional non-homogeneous boundary condition

$$(\mathbf{n}\cdot\boldsymbol{\epsilon}(\mathbf{u}))\times\mathbf{n}_{|\Gamma} = (\mathbf{n}\cdot\boldsymbol{\epsilon}(\mathbf{u}_P))\times\mathbf{n}_{|\Gamma}. \tag{3.7}$$

That is, we want the tangential component of the normal stress to be equal to that of the Poincaré solution. As mentioned in [10], it is clear that

Claim 3.1 (*See [10]*). *$\mathbf{u}_P$ is a steady state solution of (3.2)–(3.3) – (3.5)–(3.7).*

3.2. Long term stability

The question that we now want to investigate is whether there is a threshold on ν beyond which $\mathbf{u}_P$ is a stable solution as $t \to +\infty$; i.e., does the flow return to $\mathbf{u}_P$ independently of the initial data as $t \to +\infty$ if ν is large enough. We show in this section that the answer to this question is no, the fundamental reason being that rigid-body rotations cannot be dampened by viscous dissipation, no matter how large ν is.

Proposition 3.1. (i) *For all $\nu > 0$, $\{\mathbf{u}_P\}$ is not an attractor of the Navier–Stokes problem (3.2)–(3.3) equipped with the boundary conditions (3.5)–(3.7).*

(ii) *$\{\mathbf{u}_P\} + \mathcal{R}$ is the global attractor if $\varepsilon/\nu < 2K$ where K is the Korn constant introduced in Lemma 2.2, and the convergence to the attractor is exponential.*

Proof. Let us first prove item (i). Let $\rho > 0$ be an arbitrary positive number. Let $\mathbf{B}(\mathbf{u}_P, \rho) \subset \mathbf{H}$ be a ball of radius ρ centered at $\mathbf{u}_P$. Let $\mathbf{w} = \omega\mathbf{e}_z \times \mathbf{r}$ be a rigid-body rotation about the Oz-axis, and assume that $\omega \neq 0$ is small enough so that $\mathbf{u}_P + \mathbf{w} \in \mathbf{B}(\mathbf{u}_P, \rho)$. Let us prove that $\mathbf{u}_P + \mathbf{w}$ is a steady state solution of (3.2)–(3.3)–(3.5)–(3.7). Owing to $\boldsymbol{\epsilon}(\mathbf{w}) = 0$, $\mathbf{w}\cdot\mathbf{n}_{|\Gamma} = 0$, $\nabla\cdot\mathbf{w} = 0$, it is clear that $\mathbf{u}_P + \mathbf{w}$ is solenoidal and satisfies the boundary conditions (3.5)–(3.7). Let us now show that it is possible to find a pressure field so that the steady state momentum equation holds. Let us first prove that $\mathbf{u}_P\cdot\nabla\mathbf{w} + \mathbf{w}\cdot\nabla\mathbf{u}_P + 2\varepsilon\mathbf{e}_x \times \mathbf{w}$ is a gradient. A straightforward computation gives:

$$\mathbf{u}_P\cdot\nabla\mathbf{w} = \omega\begin{pmatrix}\frac{2\varepsilon}{\beta}(1+\beta)z - x\\ -y\\ 0\end{pmatrix}, \qquad \mathbf{w}\cdot\nabla\mathbf{u}_P = \omega\begin{pmatrix}-x\\ -y\\ \frac{2\varepsilon}{\beta}x\end{pmatrix},$$

$$2\varepsilon\mathbf{e}_x \times \mathbf{w} = \omega\begin{pmatrix}0\\ 0\\ 2\varepsilon x\end{pmatrix},$$

so that

$$\mathbf{u}_P\cdot\nabla\mathbf{w} + \mathbf{w}\cdot\nabla\mathbf{u}_P + 2\varepsilon\mathbf{e}_x\times\mathbf{w} = -\nabla\left(\omega(x^2+y^2)\right) + \nabla\left(\frac{2\varepsilon\omega}{\beta}(1+\beta)xz\right). \tag{3.8}$$

Let us then define $q(\mathbf{x}) := -\omega(x^2+y^2) + \frac{2\varepsilon\omega}{\beta}(1+\beta)xz$. Observe that we can define the pressure field $r(\mathbf{x})$ so that $\nabla r := -\mathbf{u}_P\cdot\nabla\mathbf{u}_P - 2\varepsilon\mathbf{e}_x \times \mathbf{u}_P$, since $\mathbf{u}_P$ solves (3.2). Let us finally observe that

$$\mathbf{w}\cdot\nabla\mathbf{w} = -\frac{1}{2}\nabla|\mathbf{w}|^2. \tag{3.9}$$

Then we conclude that $\mathbf{u}_P + \mathbf{w}$ solves Eq. (3.2) with $p = q + r - \frac{1}{2}|\mathbf{w}|^2$. In particular if we set $\mathbf{u}_0 = \mathbf{u}_P + \mathbf{w}$, then $\mathbf{u}_P + \mathbf{w}$ remains a solution forever, i.e., the solution does not converge to $\mathbf{u}_P$ as $t \to +\infty$, no matter how small ρ is and no matter how large ν is. This proves that although $\{\mathbf{u}_P\}$ is an invariant set, it is not an attracting set.

We now prove item (ii). Let $\mathbf{u} \in L^2((0,+\infty);\mathbf{L}^2(\Omega)) \cap L^\infty((0,+\infty);\mathbf{H}^1(\Omega))$ be a Leray–Hopf solution of (3.2)–(3.3)–(3.5)–(3.7). Similarly to what has been done in the proof of Proposition 2.3 we consider the following decomposition

$$\mathbf{u}(t) - \mathbf{u}_P = \mathbf{u}^\perp(t) + \lambda(t)\mathbf{e}_z \times \mathbf{x}, \quad \text{where} \quad \mathbf{u}^\perp(t) \in \mathcal{R}^\perp,\ \lambda(t)\in\mathbb{R},\ \forall t\in[0,+\infty),$$

and let us denote $\mathbf{w} = \lambda(t)\mathbf{e}_z \times \mathbf{x}$. Upon testing the momentum equation with $\mathbf{u}^\perp(t)$ we formally obtain:

$$\frac{1}{2}\|\mathbf{u}^\perp(t_2)\|^2_{\mathbf{L}^2(\Omega)} - \frac{1}{2}\|\mathbf{u}^\perp(t_1)\|^2_{\mathbf{L}^2(\Omega)} + 2\nu\int_{t_1}^{t_2}\|\boldsymbol{\epsilon}(\mathbf{u}^\perp(t))\|^2_{\mathbf{L}^2(\Omega)}\,\mathrm{d}t + \int_{t_1}^{t_2}\int_\Omega ((\mathbf{u}-\mathbf{u}_P)\cdot\nabla\mathbf{u} + \mathbf{u}_P\cdot\nabla(\mathbf{u}-\mathbf{u}_P) + 2\varepsilon\mathbf{e}_x\times(\mathbf{u}-\mathbf{u}_P))\cdot\mathbf{u}^\perp(t)\,\mathrm{d}\mathbf{x}\,\mathrm{d}t \le 0.$$

A rigorous proof would require a passage to the limit à la Sell [15, Section 2.3]. Using the decomposition $\mathbf{u} - \mathbf{u}_P = \mathbf{u}^\perp + \mathbf{w}$ together with (3.8) and (3.9), we obtain

$$\frac{1}{2}\|\mathbf{u}^\perp(t_2)\|^2_{\mathbf{L}^2(\Omega)} - \frac{1}{2}\|\mathbf{u}^\perp(t_1)\|^2_{\mathbf{L}^2(\Omega)} + 2K\nu\int_{t_1}^{t_2}\|\mathbf{u}^\perp(t)\|^2_{\mathbf{L}^2(\Omega)}\,\mathrm{d}t + \int_{t_1}^{t_2}\int_\Omega\left(\mathbf{u}^\perp(t)\cdot\nabla(\mathbf{u}_P+\mathbf{w})\cdot\mathbf{u}^\perp(t)\right)\mathrm{d}\mathbf{x}\,\mathrm{d}t \le 0.$$

Using that $\mathbf{v}\cdot\nabla\mathbf{w}\cdot\mathbf{v}=0$ for any vector field $\mathbf{v}$, we finally infer the following energy estimate:

$$\frac{1}{2}\|\mathbf{u}^{\perp}(t_2)\|^2_{\mathbf{L}^2(\Omega)}-\frac{1}{2}\|\mathbf{u}^{\perp}(t_1)\|^2_{\mathbf{L}^2(\Omega)}+2K\nu\int_{t_1}^{t_2}\|\mathbf{u}^{\perp}(t)\|^2_{\mathbf{L}^2(\Omega)}\,\mathrm{d}t$$
$$-2\varepsilon\int_{t_1}^{t_2}\int_{\Omega}u_y^{\perp}(t)u_z^{\perp}(t)\,\mathrm{d}\mathbf{x}\,\mathrm{d}t\le 0,$$

where we used $\mathbf{v}\cdot\nabla\mathbf{u}_P\cdot\mathbf{v}=-2\varepsilon v_y v_z$ for any vector field $\mathbf{v}$. Then using Lemma 4.1 and assuming that $\varepsilon/\nu<2K$, we conclude that $\|\mathbf{u}^{\perp}(t)\|^2_{\mathbf{L}^2(\Omega)}\le\|\mathbf{u}_0^{\perp}\|^2_{\mathbf{L}^2(\Omega)}e^{-2(2K\nu-\varepsilon)t}$. Using (3.13), we deduce that

$$(\lambda(t_2)-\lambda(t_1))\int_{\Omega}(\mathbf{e}_z\times\mathbf{x})^2$$
$$=-\varepsilon\int_{t_1}^{t_2}\int_{\Omega}\mathbf{e}_y\cdot(\mathbf{x}\times(\lambda(\tau)(\mathbf{e}_z\times\mathbf{x})+\mathbf{u}^{\perp})).$$

But Lemma 3.2 implying that

$$\int_{\Omega}\mathbf{e}_y\cdot(\mathbf{x}\times(\lambda(\tau)(\mathbf{e}_z\times\mathbf{x})))=\lambda(\tau)\int_{\Omega}\mathbf{e}_y\cdot(\mathbf{x}\times(\mathbf{e}_z\times\mathbf{x}))$$
$$=2\lambda(\tau)\int_{\Omega}(\mathbf{e}_z\times\mathbf{x})\cdot(\mathbf{e}_x\times(\mathbf{e}_z\times\mathbf{x}))=0,$$

we finally infer that

$$|\lambda(t_2)-\lambda(t_1)|\int_{\Omega}(\mathbf{e}_z\times\mathbf{x})^2\le\varepsilon\int_{t_1}^{t_2}\int_{\Omega}|\mathbf{e}_y\cdot(\mathbf{x}\times\mathbf{u}^{\perp})|$$
$$\le c\mu^{-1}\left(e^{-\mu t_1}-e^{-\mu t_2}\right),$$

where c is a generic constant and $\mu:=2K\nu-\varepsilon$. This immediately implies that $\lambda(t)$ converges exponentially to a constant. In conclusion $\mathbf{u}(t)-\mathbf{u}_P$ converges exponentially fast to an element in $\mathcal{R}$ as t tends to infinity. □

Remark 3.1. Proposition 3.1 is the generalization of Proposition 2.3 with $\varepsilon\neq 0$. Item (ii) of Proposition 3.1 is similar in spirit to the result of Stewartson and Roberts [18].

3.3. Angular momentum balance

Let us now mention a result on the balance of the angular momentum. Let us assume that $\mathbf{u}$ solves (3.2)–(3.3) with the boundary conditions

$$\mathbf{n}\cdot\mathbf{u}=0\quad\text{on }\Gamma,\tag{3.10}$$
$$(\mathbf{n}\cdot\boldsymbol{\epsilon}(\mathbf{u}))\times\mathbf{n}=\mathbf{g}\times\mathbf{n}\quad\text{on }\Gamma,\tag{3.11}$$

where the field $\mathbf{g}$ is a boundary data. Let us now define the angular momentum

$$\mathbf{M}:=\int_{\Omega}\mathbf{x}\times\mathbf{u}.\tag{3.12}$$

Lemma 3.1. *Denoting by M_z and M_y the z- and y-component of* $\mathbf{M}$, *respectively, all the weak solutions of* (3.2)–(3.3)–(3.10)–(3.11) *satisfy*

$$\partial_t M_z+\varepsilon M_y$$
$$=-\int_{\Gamma}\nu(\mathbf{g}\times\mathbf{n})\cdot((\mathbf{e}_z\times\mathbf{x})\times\mathbf{n}),\quad a.e.\ t\in(0,+\infty).\tag{3.13}$$

Proof. Observing that $M_z=\int_{\Omega}(\mathbf{e}_z\times\mathbf{x})\cdot\mathbf{u}$, we multiply (3.2) by $\mathbf{e}_z\times\mathbf{x}$ and integrate over Ω. Using the divergence free condition together with (3.10) and integrating by parts, we infer that

$$\int_{\Omega}(\mathbf{e}_z\times\mathbf{x})\cdot(\mathbf{u}\cdot\nabla\mathbf{u})=\int_{\Omega}\nabla\cdot(\mathbf{u}\otimes\mathbf{u})\cdot(\mathbf{e}_z\times\mathbf{x})$$
$$=\int_{\Gamma}(\mathbf{u}\cdot\mathbf{n})\,(\mathbf{u}\cdot(\mathbf{e}_z\times\mathbf{x}))=0,$$

where we used that $(\mathbf{u}\otimes\mathbf{u}):\nabla(\mathbf{e}_z\times\mathbf{x})=0$ since the matrix $\mathbf{u}\otimes\mathbf{u}$ is symmetric and $\nabla(\mathbf{e}_z\times\mathbf{x})$ is anti-symmetric. The same argument applies to the viscous term

$$\int_{\Omega}(\mathbf{e}_z\times\mathbf{x})\cdot\nu\nabla\cdot(\boldsymbol{\epsilon}(\mathbf{u}))=\int_{\Gamma}\nu(\boldsymbol{\epsilon}(\mathbf{u})\cdot\mathbf{n})\cdot(\mathbf{e}_z\times\mathbf{x})$$
$$=\int_{\Gamma}\nu(\mathbf{g}\times\mathbf{n})\cdot((\mathbf{e}_z\times\mathbf{x})\times\mathbf{n}),$$

where we used $\mathbf{e}_z\times\mathbf{x}=(\mathbf{e}_z\times\mathbf{x})\times\mathbf{n}$ since $(\mathbf{e}_z\times\mathbf{x})\cdot\mathbf{n}_{|\Gamma}=0$. The same argument applies again for the pressure term since $\nabla p=\nabla\cdot(pI)$ where I is the identity matrix.

$$\int_{\Omega}(\mathbf{e}_z\times\mathbf{x})\cdot\nabla p=\int_{\Gamma}p(\mathbf{e}_z\times\mathbf{x})\cdot\mathbf{n}=0.$$

We now deal with the Coriolis term by applying Lemma 3.2:

$$\int_{\Omega}(\mathbf{e}_z\times\mathbf{x})\cdot(\mathbf{e}_x\times\mathbf{u})=\frac{1}{2}\int_{\Omega}\mathbf{e}_y\cdot(\mathbf{x}\times\mathbf{u})=\frac{1}{2}M_y.$$

The conclusion follows readily. □

Lemma 3.2. *Let* $\mathbf{v}\in\mathbf{L}^1(\Omega)$ *be an integrable vector field such that* $\nabla\cdot\mathbf{v}=0$ *and* $\mathbf{v}\cdot\mathbf{n}_{|\Gamma=0}$, *then*

$$\int_{\Omega}\mathbf{e}_y\cdot(\mathbf{x}\times\mathbf{v})=2\int_{\Omega}(\mathbf{e}_z\times\mathbf{x})\cdot(\mathbf{e}_x\times\mathbf{v}).\tag{3.14}$$

Proof. Let us first observe that $\int_{\Omega}(\mathbf{e}_z\times\mathbf{x})\cdot(\mathbf{e}_x\times\mathbf{v})=-\int_{\Omega}xv_z$. Noticing that $\int_{\Omega}xv_z+zv_x=\int_{\Omega}\mathbf{v}\cdot\nabla(zx)=0$ since $\nabla\cdot\mathbf{v}=0$ and $\mathbf{v}\cdot\mathbf{n}_{|\Gamma}=0$, we infer that

$$\int_{\Omega}(\mathbf{e}_z\times\mathbf{x})\cdot(\mathbf{e}_x\times\mathbf{v})=-\int_{\Omega}xv_z=\frac{1}{2}\int_{\Omega}zv_x-xv_z$$
$$=\frac{1}{2}\int_{\Omega}\mathbf{e}_y\cdot(\mathbf{x}\times\mathbf{v}),$$

which concludes the proof. □

Remark 3.2. If we choose $\mathbf{g}=\boldsymbol{\epsilon}(\mathbf{u}_P)\cdot\mathbf{n}$ like in Eq. (3.7), then $-\int_{\Gamma}\nu(\mathbf{g}\times\mathbf{n})\cdot((\mathbf{e}_z\times\mathbf{x})\times\mathbf{n})$ is equal to $-\int_{\Omega}(\mathbf{e}_z\times\mathbf{x})\cdot\nu\nabla\cdot(\boldsymbol{\epsilon}(\mathbf{u}_P))=0$ and the balance equation of the angular momentum in the z direction simplifies to $\partial_t M_z+\varepsilon M_y=0$.

Remark 3.3. Note that (3.13) is just a consequence of (3.2)–(3.3)–(3.10)–(3.11). This balance holds whether the long term stability of (3.2)–(3.3)–(3.10)–(3.11) is spurious or not. It is false to consider that (3.13) is an additional equation that fixes the long term stability behavior of the system.

4. Precession driven flow with stress-free boundary conditions

We show in this section that if we enforce $(\mathbf{n}\cdot\boldsymbol{\epsilon}(\mathbf{u}))\times\mathbf{n}_{|\Gamma}=0$, instead of enforcing $(\mathbf{n}\cdot\boldsymbol{\epsilon}(\mathbf{u}))\times\mathbf{n}_{|\Gamma}=(\mathbf{n}\cdot\boldsymbol{\epsilon}(\mathbf{u}_P))\times\mathbf{n}_{|\Gamma}$ in (3.2)–(3.3)–(3.10), then 0 becomes the unique stable solution as $t\to+\infty$, i.e., $\{0\}$ is the global attractor.

4.1. Long time stability

The setting of the problem is the same as in Section 3.1 except that we enforce the tangential component of the normal stress to be zero at the boundary.

$$\partial_t \mathbf{u} + \mathbf{u}\cdot\nabla\mathbf{u} - 2\nu\nabla\cdot\boldsymbol{\epsilon}(\mathbf{u}) + 2\varepsilon\mathbf{e}_x\times\mathbf{u} + \nabla p = 0 \quad \text{in } \Omega \tag{4.1}$$

$$\nabla\cdot\mathbf{u} = 0 \quad \text{in } \Omega \tag{4.2}$$

$$\mathbf{n}\cdot\mathbf{u} = 0 \quad \text{on } \Gamma \tag{4.3}$$

$$(\mathbf{n}\cdot\boldsymbol{\epsilon}(\mathbf{u}))\times\mathbf{n} = 0 \quad \text{on } \Gamma \tag{4.4}$$

$$\mathbf{u}_{|t=0} = \mathbf{u}_0 \quad \text{in } \Omega. \tag{4.5}$$

The result that we want to emphasize is that contrary to what we observed in Section 3, 0 becomes the unique stable solution of (4.1)–(4.5) as $t \to +\infty$. The main result that we want to prove here is that any solution of the system (4.1)–(4.4) returns to rest as $t \to +\infty$. This fact has been mentioned in [10] without proof. The key argument is that rigid-body rotations about the Oz axis are not stationary solutions of (4.1).

Theorem 4.1. $\{0\}$ *is the global attractor of* (4.1)–(4.5)*.*

Proof. Let us start by observing that $\{0\}$ is indeed an invariant set of (4.1)–(4.5). Let $\mathbf{B}(0,\rho)$ be the unit ball in $\mathbf{H}$ centered at 0 and of radius ρ. Let $\mathbf{u}_0 \in \mathbf{B}(0,\rho)$ and let $\mathbf{u} \in L^2((0,+\infty);\mathbf{L}^2(\Omega)) \cap L^\infty((0,+\infty);\mathbf{H}^1(\Omega))$ be a Leray–Hopf solution of (4.1)–(4.5) and consider the following decomposition:

$$\mathbf{u}(t) = \mathbf{u}^\perp(t) + \lambda(t)\mathbf{e}_z\times\mathbf{x}, \quad \text{where} \quad \mathbf{u}^\perp(t) \in \mathcal{R}^\perp,\ \lambda(t)\in\mathbb{R},\ \forall t\in[0,+\infty).$$

Lemma 2.2 together with $\mathbf{u}$ being a Leray–Hopf solution implies that

$$\|\mathbf{u}^\perp(t)\|^2_{\mathbf{L}^2(\Omega)} + c_z\lambda(t)^2 + 4\nu K\int_0^t \|\mathbf{u}^\perp(\tau)\|^2_{\mathbf{L}^2(\Omega)}\,d\tau \le \|\mathbf{u}_0\|^2_{\mathbf{L}^2(\Omega)}$$

where $c_z = \|\mathbf{e}_z\times\mathbf{x}\|^2_{\mathbf{L}^2}$ (recall $t \longmapsto \mathbf{u}(t)$ is continuous in the $\mathbf{L}^2$-weak topology). Let $t_2 > t_1$ in $(0,+\infty)$, then (3.13) means that

$$\begin{aligned}|\lambda(t_2)-\lambda(t_1)|\int_\Omega(\mathbf{e}_z\times\mathbf{x})^2 &\le \varepsilon\int_{t_1}^{t_2}\int_\Omega|(\mathbf{e}_y\times\mathbf{x})\cdot\mathbf{u}|\\ &\le \varepsilon|t_2-t_1|\|\mathbf{u}_0\|_{\mathbf{L}^2}\|(\mathbf{e}_y\times\mathbf{x})\|_{\mathbf{L}^2},\end{aligned}$$

thereby proving that $t \longmapsto \lambda(t)$ is uniformly Lipschitz over $(0,+\infty)$. Since $\mathbf{u}$ is a Leray–Hopf solution we also have

$$\|\mathbf{u}^\perp(t_2)\|^2_{\mathbf{L}^2} - \|\mathbf{u}^\perp(t_1)\|^2_{\mathbf{L}^2} + (\lambda(t_2)^2-\lambda(t_1)^2)\|\mathbf{e}_z\times\mathbf{x}\|^2_{\mathbf{L}^2} + 4\nu\int_{t_1}^{t_2}\int_\Omega|\boldsymbol{\epsilon}(\mathbf{u})|^2 \le 0.$$

This in turn implies that

$$\begin{aligned}&\frac{\|\mathbf{u}^\perp(t_2)\|^2_{\mathbf{L}^2} - \|\mathbf{u}^\perp(t_1)\|^2_{\mathbf{L}^2}}{t_2-t_1}\\ &\le (|\lambda(t_2)+\lambda(t_1)|)\frac{|\lambda(t_2)-\lambda(t_1)|}{|t_2-t_1|}\|\mathbf{e}_z\times\mathbf{x}\|^2_{\mathbf{L}^2}\\ &\le 2\varepsilon\|\mathbf{u}_0\|^2_{\mathbf{L}^2}\|\mathbf{e}_y\times\mathbf{x}\|_{\mathbf{L}^2}\|\mathbf{e}_z\times\mathbf{x}\|^{-1}_{\mathbf{L}^2} =: \gamma.\end{aligned}$$

In conclusion the function $t \longmapsto \|\mathbf{u}^\perp(t)\|^2_{\mathbf{L}^2}$ satisfies the assumptions of Lemma 4.2. We then infer that $\|\mathbf{u}^\perp\|_{L^\infty((t,+\infty);\mathbf{L}^2)} \to 0$ as $t \to +\infty$.

Let $\delta > 0$ be an arbitrarily small number. Let t_δ be so that $\|\mathbf{u}^\perp\|_{L^\infty((t,+\infty);\mathbf{L}^2)} \le \delta$ for all $t \ge t_\delta$. Let $t_2 > t_1 \ge t_\delta$ in $(0,+\infty)$ then the energy balance implies

$$\|\mathbf{u}^\perp(t_2)\|^2_{\mathbf{L}^2} + c_z\lambda(t_2)^2 \le \|\mathbf{u}^\perp(t_1)\|^2_{\mathbf{L}^2} + c_z\lambda(t_1)^2,$$

which also gives

$$\lambda(t_2)^2 \le \lambda(t_1)^2 + 2c_z^{-1}\delta^2.$$

Lemma 4.3 in turn implies that $\lambda(t)$ converges to real a number λ_∞ as t goes to infinity, since λ is a continuous function. Using (3.13) again, we infer that

$$\begin{aligned}&(\lambda(t_2)-\lambda(t_1))\int_\Omega(\mathbf{e}_z\times\mathbf{x})^2\\ &= -\varepsilon\int_{t_1}^{t_2}\int_\Omega \mathbf{e}_y\cdot(\mathbf{x}\times(\lambda(\tau)(\mathbf{e}_z\times\mathbf{x})+\mathbf{u}^\perp)).\end{aligned}$$

But Lemma 3.2 implying that

$$\begin{aligned}&\int_\Omega \mathbf{e}_y\cdot(\mathbf{x}\times(\lambda(\tau)(\mathbf{e}_z\times\mathbf{x}))) = \lambda(\tau)\int_\Omega \mathbf{e}_y\cdot(\mathbf{x}\times(\mathbf{e}_z\times\mathbf{x}))\\ &= 2\lambda(\tau)\int_\Omega(\mathbf{e}_z\times\mathbf{x})\cdot(\mathbf{e}_x\times(\mathbf{e}_z\times\mathbf{x})) = 0,\end{aligned}$$

we finally infer that

$$\begin{aligned}|\lambda(t_2)-\lambda(t_1)|\int_\Omega(\mathbf{e}_z\times\mathbf{x})^2 &\le \varepsilon\int_{t_1}^{t_2}\int_\Omega|\mathbf{e}_y\cdot(\mathbf{x}\times\mathbf{u}^\perp)|\\ &\le c\delta|t_2-t_1|,\end{aligned}$$

where c is a generic constant that depends on Ω and may vary at each occurrence from now on. Let us take $\boldsymbol{\varphi} \in \mathcal{D}(\Omega)$ independent of time and divergence-free. Since $\mathbf{u}$ is a Leray solution we have

$$\begin{aligned}0 &= \int_\Omega(\mathbf{u}(t_2,\mathbf{x})-\mathbf{u}(t_1,\mathbf{x}))\cdot\boldsymbol{\varphi}(\mathbf{x})\,d\mathbf{x}\\ &\quad+\int_{t_1}^{t_2}\int_\Omega 2\varepsilon\mathbf{u}(\tau,\mathbf{x})\cdot(\boldsymbol{\varphi}(\mathbf{x})\times\mathbf{e}_x)\,d\mathbf{x}\,d\tau\\ &\quad-\int_{t_1}^{t_2}\int_\Omega 2\nu\mathbf{u}(\tau,\mathbf{x})\cdot\nabla\cdot\boldsymbol{\epsilon}(\boldsymbol{\varphi})\,d\mathbf{x}\,d\tau\\ &\quad-\int_{t_1}^{t_2}\int_\Omega(\mathbf{u}(\mathbf{x})\otimes\mathbf{u}(\mathbf{x})):\nabla\boldsymbol{\varphi}(\mathbf{x})d\mathbf{x}\,d\tau.\end{aligned}$$

Let us now set $t_2 = t_1+1$. Upon observing that $\int_\Omega((\mathbf{e}_z\times\mathbf{x})\otimes(\mathbf{e}_z\times\mathbf{x})):\nabla\boldsymbol{\varphi}(\mathbf{x})d\mathbf{x} = 0$ and $\int_\Omega(\mathbf{e}_z\times\mathbf{x})\cdot\nabla\cdot\boldsymbol{\epsilon}(\boldsymbol{\varphi})\,d\mathbf{x} = 0$. This implies that there is a constant $c(\boldsymbol{\varphi}) \ge 0$ so that

$$\begin{aligned}&2\varepsilon\left|\int_{t_1}^{t_2}\lambda(\tau)\,d\tau\int_\Omega(\mathbf{e}_z\times\mathbf{x})\cdot(\boldsymbol{\varphi}(\mathbf{x})\times\mathbf{e}_x)\,d\mathbf{x}\right|\\ &\le\left|(\lambda(t_2)-\lambda(t_1))\int_\Omega(\mathbf{e}_z\times\mathbf{x})\cdot\boldsymbol{\varphi}(\mathbf{x})\,d\mathbf{x}\right| + c(\boldsymbol{\varphi})\delta.\end{aligned}$$

Let us choose $\boldsymbol{\varphi}$ so that $2\varepsilon\int_\Omega(\mathbf{e}_z\times\mathbf{x})\cdot(\boldsymbol{\varphi}(\mathbf{x})\times\mathbf{e}_x)\,d\mathbf{x} = 1$. The above estimate implies that

$$\left|\int_{t_1}^{t_1+1}\lambda(\tau)\,d\tau\right| \le c(\boldsymbol{\varphi})\delta.$$

This implies that $\lambda_\infty = \lim_{t_1\to\infty}\int_{t_1}^{t_1+1}\lambda(\tau)\,d\tau \le c(\boldsymbol{\varphi})\delta$, which means that $\lambda_\infty = 0$. In conclusion

$$\lim_{t\to+\infty}\|\mathbf{u}\|_{L^\infty((t,+\infty);\mathbf{L}^2)} = 0, \tag{4.6}$$

which concludes the proof. □

4.2. Useful lemmas

We start by recalling a standard version of the Gronwall–Bellman inequality.

Lemma 4.1. *Let $u \in L^\infty((0,T);\mathbb{R}_+)$ and assume that u is lower-semi-continuous and there exists $\lambda\in\mathbb{R}$ so that the following holds*

$$u(t_2) + \lambda\int_{t_1}^{t_2}u(\tau)\,d\tau \le u(t_1), \quad \forall t_2 > t_1 > 0,$$

then

$$0 \le u(t) \le u(0)e^{-\lambda t}, \quad \forall t \in [0, T]. \tag{4.7}$$

Lemma 4.2. *Let $\alpha \in L^1((0, +\infty); \mathbb{R}_+)$ be a nonnegative integrable function. Assume that there exists a constant β so that*

$$\operatorname*{ess\,sup}_{t\neq\tau} \frac{\alpha(t) - \alpha(\tau)}{t - \tau} \le \gamma, \tag{4.8}$$

then $\lim_{t\to+\infty} \|\alpha\|_{L^\infty((t,+\infty);\mathbb{R}_+)} = 0$.

Proof. Let $M = \{t > 0, \operatorname{ess\,sup}_{t\neq\tau} \frac{\alpha(t)-\alpha(\tau)}{t-\tau} < +\infty\}$ and for all $t \in M$ let $M_t = \{\tau > 0, \sup_{t\neq\tau} \frac{\alpha(t)-\alpha(\tau)}{t-\tau} < +\infty\}$. Note that $\operatorname{meas}(\mathbb{R}_+ \setminus M) = 0$ and $\operatorname{meas}(\mathbb{R}_+ \setminus M_t) = 0$. Let us proceed by contradiction. Assume that there exists $c > 0$ so that for all $t > 0$, $\|\alpha\|_{L^\infty((t,+\infty);\mathbb{R}_+)} \ge c$. Let us set $t_0 = 0$. Since α is integrable, there is a set $A_1^* \subset (t_0 + 1, +\infty)$ of positive measure and diameter 1 so that $\alpha(\tau) \le \frac{1}{2}c$, for all τ in A_1^*. Let $t_1^* \in A_1^* \cap M$ (note that this set cannot be empty). Then, there is set $A_1 \subset (t_1^* + 1, \infty)$ of positive measure and diameter 1 so that $\alpha(\tau) \ge \frac{3}{4}c$, for all τ in A_1. Let $t_1 \in A_1 \cap M_{t_1^*}$ (note that this set cannot be empty). By repeating the above argument we construct an increasing sequence $t_1^* < t_1 < t_2^* < t_2 < \cdots$ Note that the hypothesis $(\alpha(t_i)-\alpha(t_i^*))/(t_i-t_i^*) \le \gamma$ implies that $t_i - t_i^* \ge c/(4\gamma)$ for all $i \ge 1$. Let us consider the time $\hat{t}_i := t_i - c/4\gamma \ge t_i^* > t_{i-1}$. The following holds owing to (4.8)

$$\frac{c}{2} \le \frac{3c}{4} - \frac{c}{4} \le \alpha(t_i) - \gamma(t_i - \tau) \le \alpha(\tau), \quad \text{a.e. } \tau \in (\hat{t}_i, t_i).$$

This means that $\int_{\hat{t}_i}^{t_i} \alpha(\tau)\,d\tau \ge \frac{c^2}{8\gamma}$ for all $\hat{t}_i$, which contradicts the fact that α is integrable. □

Lemma 4.3. *Let $\psi \in \mathcal{C}^0([0, +\infty); \mathbb{R}_+)$ so that for all $\delta > 0$ there is $t_\delta \ge 0$ so that for all $t_2 \ge t_1 \ge t_\delta$, $\psi(t_1) + \delta \ge \psi(t_2)$, then $\psi(t)$ converges to a finite limit as t goes to infinity.*

Proof. Let $\overline{\psi} := \limsup_{t\ge 0} \psi(t)$ and $\underline{\psi} := \liminf_{t\ge 0} \psi(t)$. Let $\delta > 0$ be a positive real number. There are $t_1 \ge t_\delta$ and $t_2 \ge t_1 \ge t_\delta$ so that

$$\psi(t_1) \le \underline{\psi} + \delta, \quad \text{and} \quad \overline{\psi} - \delta \le \psi(t_2),$$

which in turn implies that

$$\overline{\psi} - \delta \le \psi(t_2) \le \psi(t_1) + \delta \le \underline{\psi} + 2\delta.$$

In conclusion $\overline{\psi} \le \underline{\psi} + 3\delta$, which implies $\overline{\psi} = \underline{\psi}$ since δ is arbitrary. This completes the proof. □

5. Numerical illustrations

We now illustrate the mathematical results from Section 3–4 by performing numerical simulations with the geometry used in [10]. The simulations are performed using the SFEMaNS code [19] which has been extensively validated on precession flows [11]. The authors of [10] study the dynamo action in an oblate spheroid defined by Eq. (3.1) with $\beta = 0.5625$ (this corresponds to the value $b = 0.8$ for the semi-minor axis used in [10], $b := (1 + \beta)^{-\frac{1}{2}}$). This spheroid rotates about the Oz-axis and precesses about the Ox-axis with a precession rate ε. Two sets of boundary conditions are considered: either the homogeneous stress-free boundary or the Poincaré stress condition is enforced. The normalization is done so that the Reynolds number is equal to ν^{-1}.

5.1. Stress-free boundary condition

The first simulation solves the equations (4.1)–(4.2)–(4.3)–(4.4) with stress-free boundary conditions using the initial data $\mathbf{u}_{|t=0} = 0.1\mathbf{e}_z \times \mathbf{x} = 0.1(-y\mathbf{e}_x + x\mathbf{e}_y)$. The normalized viscosity is $\nu = 0.024$ and the precession rate is $\varepsilon = 0.25$ as in [10]. The left panel in Fig. 1 shows the time derivative of the total energy $E_K = \frac{1}{2}\|\mathbf{u}\|^2_{\mathbf{L}^2}$ in the precessing frame. Note that $\partial_t E_K$ is always negative, establishing that E_K is a decreasing function. This graph is in excellent agreement with Fig. 1(a) of [10]. It also shows that $\mathbf{u} \to 0$ as $t \to \infty$ in agreement with (4.6) (i.e., $\{0\}$ is indeed the global attractor). The right panel in the figure shows the time derivative of the angular momentum along the Oz-axis and the quantity $50(\partial_t M_z + \varepsilon M_y)$ evaluated numerically at each time step (see Lemma 3.1). We observe that $\partial_t M_z + \varepsilon M_y$ is zero up to truncation errors as expected. This graph is also in excellent agreement with Fig. 1(b) of [10].

5.2. Poincaré stress boundary condition

5.2.1. Small Reynolds number flows

The second series of simulations solves equations (3.2)–(3.3)–(3.5)–(3.7) with the Poincaré stress boundary condition using different initial data and with the precession rate $\varepsilon = 0.025$. This precession rate is chosen so that ε/ν is small (with $\nu = 1$). The spatial resolution of the meridian mesh is 1/40, and 16 Fourier modes are used in the azimuthal direction. We test two different perturbations denoted PERT1 and PERT2. PERT1 corresponds to the initial condition $\mathbf{u}_0 = \mathbf{u}_P + (1 + \operatorname{rand}(r, z))\mathbf{e}_z \times \mathbf{x}$ where $\mathbf{u}_P$ is the Poincaré solution and $\operatorname{rand}(r, z)$ is a random function of amplitude in the range $[-0.5, 0.5]$. PERT2 corresponds to the initial condition $\mathbf{u}_0 = \mathbf{u}_P + \mathbf{e}_z \times \mathbf{x} + \mathbf{v}$ where $\mathbf{v}$ is a perturbation without rigid-body rotation, $\mathbf{v}(r, \theta, z) = (\frac{r}{2}\sin(\theta), r\cos(\theta), 0)$, where (r, θ, z) are the cylindrical coordinates about the Oz-axis. The y- and z-components of the angular momentum of the initial data of PERT1 are $(0, 2.67842046)$. The y- and z-components of the angular momentum of the initial data of PERT2 are $(0, 2.68077560)$. The z-component of the angular momentum is a measure of the rigid-body rotation of the initial data. Note that the z-component of the angular momentum of the initial data of PERT2 is the same as that of the rigid-body rotation $2\mathbf{e}_z \times \mathbf{x}$. We show in Figs. 2 the time evolution of the quantities $\delta E_K = \frac{1}{2}\|\mathbf{u} - \mathbf{u}_P\|^2_{\mathbf{L}^2(\Omega)}$ and $\|\mathbf{u}^\perp(t)\|_{\mathbf{L}^2(\Omega)}$ and of the y- and z-components of the angular momentum (denoted M_y and M_z in the figures, respectively). The two solutions tend to two different steady states with two different rigid-body rotations about the Oz-axis, and these rigid-body rotations are different from those of the initial data (see Fig. 2(d)). This is due to the fact that, even if the y-component of the angular momentum of the initial data is zero for both initial data, the angular momentum balance implies that the y-component of the angular momentum departs from zero when $t > 0$, thereby perturbing the z-component of the angular momentum via the conservation equation $\partial_t M_z + \varepsilon M_y = 0$ (see Fig. 2(c)). The velocity component $\mathbf{u}^\perp$ of the two steady states is zero as expected, up to truncation errors induced by the space discretization, (see Fig. 2(b)). These results illustrate the fact that, provided ε/ν is small enough, $\{\mathbf{u}_P\} + \mathcal{R}$ is the global attractor of (3.2)–(3.3)–(3.5)–(3.7), but no element in $\{\mathbf{u}_P\} + \mathcal{R}$ is an attracting set, meaning that the rigid-body rotation of the final steady state can differ from that of its initial data.

5.2.2. Large Reynolds number flows

In the third series of simulations we solve equations (3.2)–(3.3)–(3.5)–(3.7) with the Poincaré stress boundary condition at a larger Reynolds number with the precession rate $\varepsilon = 0.25$ that is used in [10]. We use $\nu = 0.00375$ and the initial data is the Poincaré solution. Fig. 3 shows the time evolution of $\delta E_K = \frac{1}{2}\|\mathbf{u} - \mathbf{u}_P\|^2_{\mathbf{L}^2(\Omega)}$ from $t = 0$ to $t = 2800$, obtained with the SFEMaNS code. The mesh size in the meridian section is of order 1/80 and 16 Fourier modes are used in the azimuthal direction. Note that contrary to what is shown in Figs. 5 and 6 of Ref. [10], the system does not converge to an oscillating state, and the order of magnitude of δE_K in our computation is at least 6 times larger than that reported in

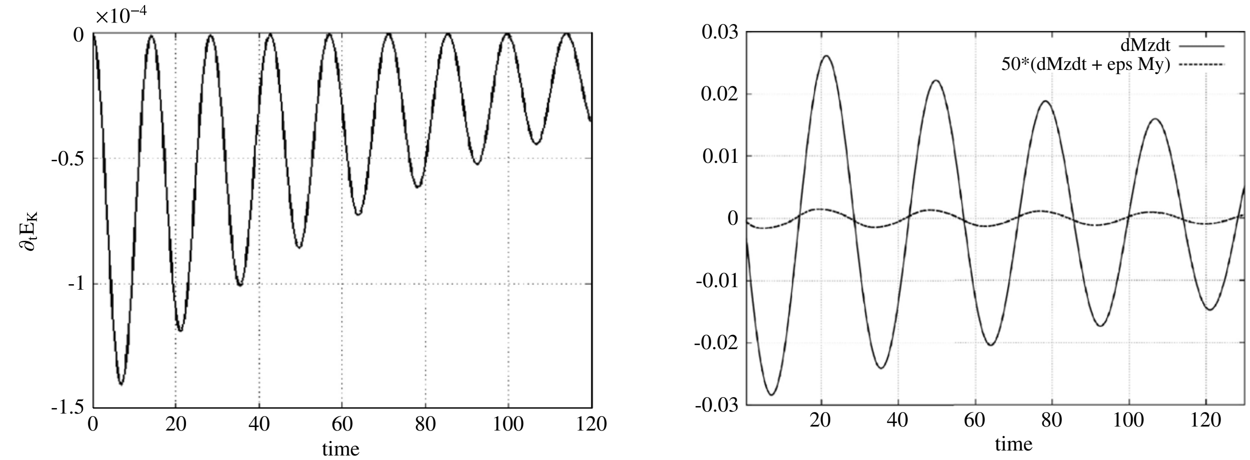

Fig. 1. Precessing spheroid with $\beta = 0.5625$, $\varepsilon = 0.25$ and $\nu = 0.024$ with the stress-free boundary condition (solution of (4.1)–(4.2)–(4.3)–(4.4)): (left) time evolution of $\partial_t E_K$ of the solution, (right) time evolution of $\partial_t M_z$ and $50(\partial_t M_z + \varepsilon M_y)$.

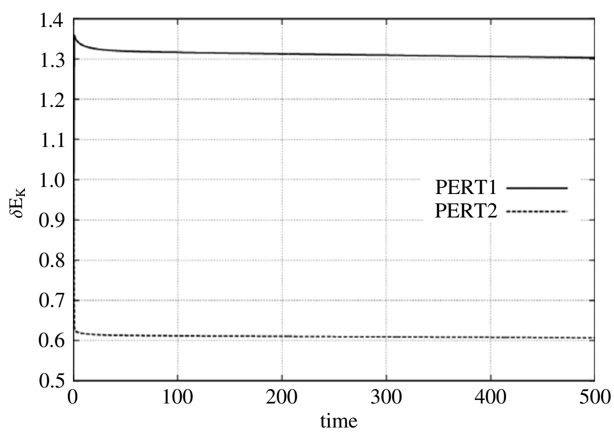

(a) δE_K vs. time.

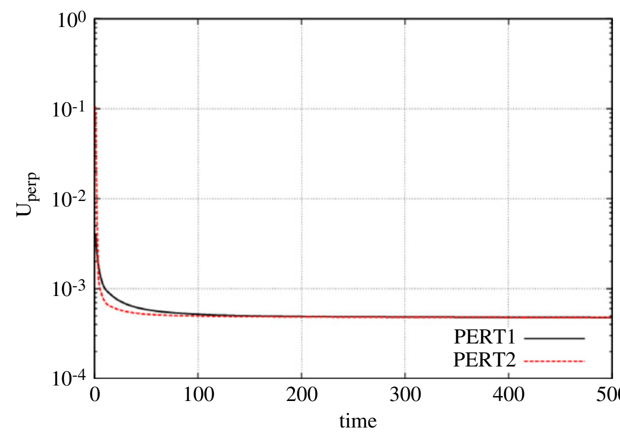

(b) $\mathbf{u}^{\perp}(t)$ vs. time.

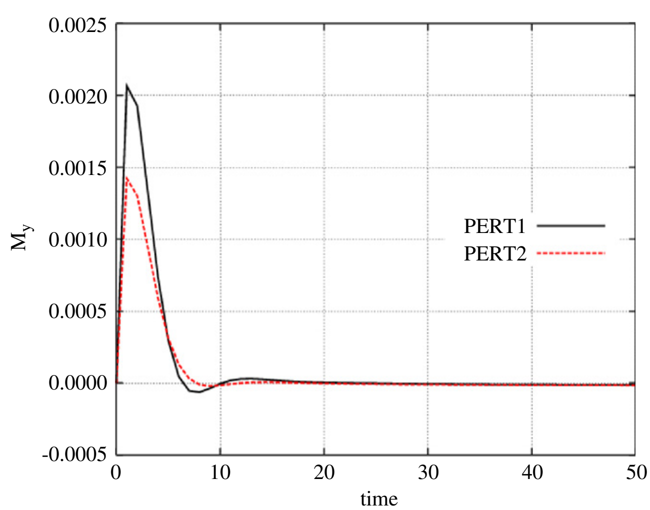

(c) M_y vs. time.

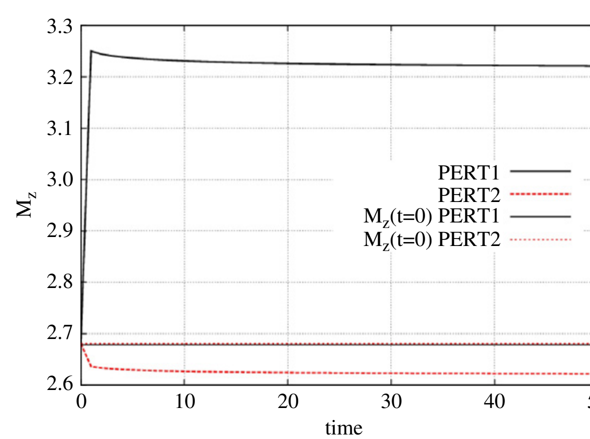

(d) M_z vs. time.

Fig. 2. (Color online) Precessing spheroid with $\beta = 0.5625$, $\varepsilon = 0.025$ and $\nu = 1$ with the Poincaré stress boundary condition (solutions of (3.2)–(3.3)–(3.5)–(3.7)). Time evolution of (a) the kinetic energy, $\delta E_K = \frac{1}{2}\|\mathbf{u} - \mathbf{u}_P\|^2_{\mathbf{L}^2(\Omega)}$, with two different perturbations (PERT1 and PERT2, see text) as initial data, (b) $\|\mathbf{u}^{\perp}(t)\|_{\mathbf{L}^2(\Omega)}$, (c) M_y, (d) M_z.

Fig. 6 of [10]. This contradictory result is reproduced by another colleague using a totally different and independent code based on a Finite Volume algorithm (S. Vantieghem, ETH, Zurich, Switzerland, personal communication). The quantity δE_K from the Finite Volume code is at least 3 times larger than that reported in Fig. 6 of [10] (data not shown). These results illustrate the fact that the attractor of (3.2)–(3.3)–(3.5)–(3.7) with the Poincaré stress boundary condition has pathological properties. The dynamo results of [10] based on the Poincaré stress boundary condition may therefore be questioned.

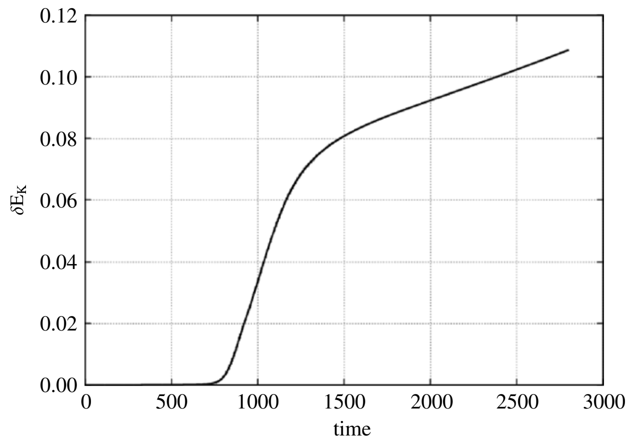

Fig. 3. Precessing spheroid with $\beta = 0.5625$, $\varepsilon = 0.25$, $\nu = 0.00375$, and the Poincaré stress boundary condition (solutions of (3.2)–(3.3)–(3.5)–(3.7)). Time evolution of the kinetic energy, $\delta E_K = \frac{1}{2}\|\mathbf{u} - \mathbf{u}_P\|^2_{\mathbf{L}^2(\Omega)}$, with the Poincaré solution as initial data.

6. Discussion

The so-called stress-free boundary condition $(\mathbf{n}\cdot\boldsymbol{\epsilon}(\mathbf{u}))\times\mathbf{n}_{|\Gamma} = 0$ is often used in the geophysics literature to avoid issues induced by viscous layers. For example, an anelastic dynamo benchmark [20] was conducted very recently in a rotating spherical shell. The authors emphasize in their concluding section the difficulties they encountered to obtain the same hydrodynamical solutions using four different codes in a model with stress-free boundary conditions applied to the ICB and the CMB. Since the container in this benchmark has the spherical symmetry (spherical shell), the balance equation (3.13) gives $\partial_t \mathbf{M} = 0$ in the inertial reference frame, and each group had to apply some remedy in order to numerically conserve the three components of the angular momentum. But, more importantly, they also had to use the same initial condition. This difficulty did not arise in the older dynamo benchmark [21] using the same geometry because the no-slip boundary condition was prescribed at the ICB and CMB.

We have proved in this work that the stress-free boundary condition with no precession leads to spurious stability behaviors when the fluid domain is axisymmetric. This problem is still present when precession is accounted for and the Poincaré stress boundary condition is imposed. One recovers stability at large times with precession when the stress-free boundary condition is enforced.

We hope that the present work will help draw the attention of the geodynamo community on this problem. The above pathological stability behaviors can be avoided by enforcing one additional condition. For instance, for problem (3.2)–(3.5) and (3.7), one could think of enforcing the vertical component of the angular momentum of the difference $\mathbf{u} - \mathbf{u}_P$, say

$$\int_\Gamma (\mathbf{u} - \mathbf{u}_P)\cdot(\mathbf{e}_z \times \mathbf{x})\,\mathrm{d}\mathbf{s} = 0, \tag{6.1}$$

or enforcing $\mathbf{u} - \mathbf{u}_P$ and $\mathbf{u}_P$ to be orthogonal in average over the boundary, say

$$\int_\Gamma (\mathbf{u} - \mathbf{u}_P)\cdot\mathbf{u}_P\,\mathrm{d}\mathbf{s} = 0. \tag{6.2}$$

For problem (2.1)–(2.5), one could think of enforcing the vertical component of the total angular momentum

$$\int_\Gamma \mathbf{u}\cdot(\mathbf{e}_z \times \mathbf{x})\,\mathrm{d}\mathbf{s} = 0, \tag{6.3}$$

as was done for the three components in the anelastic dynamo benchmark [20].

We have suggested in Section 2.4 to use a boundary condition that does not have the stability problems mentioned above. For the problem (2.1)–(2.5) this condition is

$$(\mathbf{n}\cdot\nabla\mathbf{u})\times\mathbf{n}_{|\Gamma} = 0, \tag{6.4}$$

and for the problem (3.2)–(3.5) this condition is

$$(\mathbf{n}\cdot\nabla\mathbf{u})\times\mathbf{n}_{|\Gamma} = (\mathbf{n}\cdot\nabla\mathbf{u}_P)\times\mathbf{n}_{|\Gamma}. \tag{6.5}$$

Let us finally emphasize that it is false to consider that the momentum balance equation (3.13) is an additional equation that makes (3.2)–(3.3)–(3.5)–(3.7) a well-behaved dynamical system. The Eq. (3.13) is a redundant consequence of (3.2)–(3.3)–(3.5)–(3.7). For instance, (6.1) (or (6.2) or (6.3)) is an additional equation whereas (3.13) is not.

In conclusion, using the stress boundary condition to evaluate nonlinear behaviors of Navier–Stokes systems may sometimes be dubious when the domain is axisymmetric.

Acknowledgments

The authors are happy to acknowledge helpful email discussions with P.H. Roberts and P. Boronski. They also want to thank David Cébron, Wietze Herreman, and Stijn Vantieghem for stimulating discussions. The HPC resources were provided by GENCI-IDRIS (grant 2012-0254) in France. J.-L. Guermond acknowledges support from University Paris Sud 11 and the National Science Foundation grant NSF DMS-1015984.

References

[1] G.A. Glatzmaier, P.H. Roberts, A three-dimensional self-consistent computer simulation of a geomagnetic field reversal, Nature 377 (1995) 203–209.
[2] W. Kuang, J. Bloxham, An Earth-like numerical dynamo model, Nature 389 (1997) 371–374.
[3] W. Kuang, J. Bloxham, Numerical modeling of magnetohydrodynamic convection in a rapidly rotating spherical shell: weak and strong field dynamo action, J. Comput. Phys. 153 (1) (1999) 51–81.
[4] P. Olson, Probing Earth's dynamo, Nature 389 (1997) 337–338.
[5] A. Sakuraba, P. Roberts, Generation of a strong magnetic field using uniform heat flux at the surface of the core, Nature Geosci. 2 (2009) 802–805.
[6] E. Bullard, The magnetic field within the Earth, Proc. Roy. Soc. Lond. A 197 (1051) (1949) 433–453.
[7] W.V.R. Malkus, Precession of the Earth as the Cause of Geomagnetism, Science 160 (3825) (1968) 259–264.
[8] A. Tilgner, Precession driven dynamos, Phys. Fluids 17 (3) (2005) 034104.
[9] A. Tilgner, Kinematic dynamos with precession driven flow in a sphere, Geophy. Astrophy. Fluid Dynamics 101 (1) (2007) 1.
[10] C.-C. Wu, P. Roberts, On a dynamo driven by topographic precession, Geophy. Astrophy. Fluid Dynamics 103 (6) (2009) 467–501.
[11] C. Nore, J. Léorat, J.-L. Guermond, F. Luddens, Nonlinear dynamo action in a precessing cylindrical container, Phys. Rev. E 84 (Jul) (2011) 016317.
[12] R. Mason, R. Kerswell, Chaotic dynamics in a strained rotating flow: a precessing plane fluid layer, J. Fluid Mech. 471 (2002) 71–106.
[13] J.-L. Lions, Quelques méthodes de résolution des problèmes aux limites non linéaires, volume 1. Dunod, Paris, France, 1969.
[14] R. Temam, Navier-Stokes equations, in: Theory and numerical analysis, With an appendix by F. Thomasset, third edition, in: Studies in Mathematics and its Applications, vol. 2, North-Holland Publishing Co., Amsterdam, 1984.
[15] G. Sell, Global attractors for the three-dimensional Navier–Stokes equations, J. Dynam. Differential Equations 8 (1996) 1–33. http://dx.doi.org/10.1007/BF02218613.
[16] L. Desvillettes, C. Villani, On a variant of Korn's inequality arising in statistical mechanics, ESAIM Control Optim. Calc. Var. 8 (2002) 603–619. (electronic) A tribute to J. L. Lions.
[17] G. Duvaut, J.-L. Lions, Les inéquations en mécanique et en physique. Dunod, 1972.
[18] K. Stewartson, P.H. Roberts, On the motion of liquid in a spheroidal cavity of a precessing rigid body, J. Fluid Mech. 17 (01) (1963) 1–20.
[19] J.-L. Guermond, J. Léorat, F. Luddens, C. Nore, A. Ribeiro, Effects of discontinuous magnetic permeability on magnetodynamic problems, J. Comput. Phys. 230 (2011) 6299–6319.
[20] C. Jones, P. Boronski, A. Brun, G. Glatzmaier, T. Gastine, M. Miesch, J. Wicht, Anelastic convection-driven dynamo benchmarks, Icarus 216 (1) (2011) 120–135.
[21] U. Christensen, J. Aubert, P. Cardin, E. Dormy, S. Gibbons, G. Glatzmaier, E. Grote, Y. Honkura, C. Jones, M. Kono, M. Matsushima, A. Sakuraba, F. Takahashi, A. Tilgner, J. Wicht, K. Zhang, A numerical dynamo benchmark, in: Dynamics and Magnetic Fields of the Earth's and Planetary Interiors, Physics of the Earth and Planetary Interiors 128 (1–4) (2001) 25–34.